

## Revealing Phase Transition in Dense Matter with Gravitational Wave Spectroscopy of Binary Neutron Star Mergers

PEDRO L. ESPINO,<sup>1,2</sup> AVIRAL PRAKASH,<sup>1,3</sup> DAVID RADICE,<sup>1,3,4,\*</sup> AND DOMENICO LOGOTETA<sup>5,6</sup>

<sup>1</sup>*Institute for Gravitation & the Cosmos, The Pennsylvania State University, University Park, PA 16802*

<sup>2</sup>*Department of Physics, University of California, Berkeley, CA 94720, USA*

<sup>3</sup>*Department of Physics, The Pennsylvania State University, University Park, PA 16802*

<sup>4</sup>*Department of Astronomy & Astrophysics, The Pennsylvania State University, University Park, PA 16802*

<sup>5</sup>*Dipartimento di Fisica, Università di Pisa, Largo B. Pontecorvo, 3 I-56127 Pisa, Italy*

<sup>6</sup>*INFN, Sezione di Pisa, Largo B. Pontecorvo, 3 I-56127 Pisa, Italy*

### ABSTRACT

We use numerical relativity simulations of binary neutron star mergers to show that high density deconfinement phase transitions (PTs) to quark matter can be probed using multimodal postmerger gravitational wave (GW) spectroscopy. Hadron-quark PTs suppress the one-armed spiral instability in the remnant. This is manifested in an anti-correlation between the energy carried in the  $l = 2, m = 1$  GW mode and energy density gap which separates the two phases. Consequently, a single measurement of the signal-to-noise ratios of the  $l = 2, m = 1$  and  $l = 2, m = 2$  GW modes could constrain the energy density gap of the PT.

*Keywords:* Neutron stars — Equation of state — Gravitational waves — Hydrodynamics — Instabilities

### 1. INTRODUCTION

Binary neutron star (BNS) mergers produce some of the most extreme conditions in nature, compressing matter to several times the nuclear density and to temperatures of tens of MeV (Perego et al. 2019). More extreme conditions are only found in the early Universe and in the interior of black holes (BHs). Multimessenger observations of binary neutron star (BNS) mergers can be used to probe the properties of matter in these conditions, providing a unique avenue to study the non-perturbative regime of QCD (Shibata 2005; Hinderer et al. 2010; Damour et al. 2012; Sekiguchi et al. 2011; Hotokezaka et al. 2011; Bauswein et al. 2013; Radice et al. 2017; Abbott et al. 2017a; Margalit & Metzger 2017; Bauswein et al. 2017; Radice et al. 2018b; Most et al. 2019, 2020; Bauswein et al. 2019; Coughlin et al. 2019; De et al. 2018; Abbott et al. 2019, 2018; Radice & Dai 2019; Dietrich et al. 2020; Breschi et al. 2021, 2022; Kashyap et al. 2022; Perego et al. 2022; Fujimoto et al. 2022; Prakash et al. 2021).

Presently, there are large uncertainties in the fundamental physics of strongly-interacting matter at densi-

ties of a few times nuclear saturation (Capano et al. 2020; Pang et al. 2021; Annala et al. 2022). It is not even clear what the relevant degrees of freedom are for the densities and temperatures reached in the core of remnant massive neutron stars (RMNS) of BNS mergers. It is possible that matter remains composed of nucleons, together with leptons (electrons, positrons, and muons) and photons (Perego et al. 2019; Loffredo et al. 2022). The appearance of more exotic baryons, such as hyperons, is not excluded (Sekiguchi et al. 2011; Radice et al. 2017; Logoteta 2021). It is also possible for a transition to the deconfined quark-gluon plasma phase to take place in BNS mergers (Most et al. 2019, 2020; Bauswein et al. 2019; Prakash et al. 2021). The determination of the state of matter formed in BNS mergers is one of the most pressing scientific objectives of multimessenger astronomy (Evans et al. 2021; Lovato et al. 2022).

Previous work has shown that the presence of phase transitions to deconfined quarks can be revealed by a shift of the postmerger gravitational wave (GW) peak frequency  $f_2$  from the value expected for hadronic equations of state (EOSs) (Bauswein et al. 2019; Weih et al. 2020; Blacker et al. 2020; Kedia et al. 2022). However, such frequency shifts can be degenerate with deviations

\* Alfred P. Sloan fellow

from universal relations due to hadronic physics or other effects (Most et al. 2019; Weih et al. 2020; Liebling et al. 2021; Prakash et al. 2021; Fujimoto et al. 2022; Tootle et al. 2022). It has also been suggested that the presence of a phase transition could be inferred from a measurement of the threshold mass for prompt collapse of BNS systems (Bauswein et al. 2020, 2021; Perego et al. 2022; Kashyap et al. 2022). In this *Letter*, we use 8 state-of-the-art numerical relativity simulations to show, for the first time, that the presence and strength of a QCD phase transition could be unambiguously determined through *multimodal* GW spectroscopy of RMNS. Such measurements will be possible with the next-generation of GW experiments like Cosmic Explorer (Reitze et al. 2019), Einstein Telescope (Punturo et al. 2010), and NEMO (Ackley et al. 2020).

## 2. METHODS

We consider binaries in quasi-circular orbits and eccentric encounters on nearly parabolic orbits. Although BNS mergers with highly eccentric orbits are expected to be significantly more rare than those with quasi-circular inspirals, these events may still have appreciable rates of as high as  $50 \text{ Gpc}^{-3} \text{ yr}^{-1}$  (Lee et al. 2010; Paschalidis et al. 2015); we include results from both types of mergers to consider as wide a variety of scenarios as possible. Initial data for the quasi-circular binaries is created using the conformal thin sandwich formalism (York 1999) and assuming a helical Killing vector and irrotational flows. The resulting elliptic equations are solved using the pseudo-spectral code LORENE (Gourgoulhon et al. 2001; Taniguchi et al. 2001; Taniguchi & Gourgoulhon 2002). Initial data for the eccentric encounters is constructed by superimposing two isolated, boosted, neutron stars, following Radice et al. (2016b). The initial separation of the stellar barycenters for parabolic encounters is set to 100 km, which is sufficiently large so that the level of constraint violation in the initial data is comparable to that of the quasi-circular binaries (Radice et al. 2016b).

We perform BNS merger simulations using the WhiskyTHC code (Radice & Rezzolla 2012; Radice et al. 2014a,b). WhiskyTHC makes use of the CTGamma space-time solver (Pollney et al. 2011), which is a part of the Einstein Toolkit (Zlochower et al. 2022). The adaptive mesh refinement driver Carpet (Schnetter et al. 2004) is used to generate the dynamical grid structure employed in the simulations. All simulations considered in the present work have been performed using at least two grid resolutions. Although there are quantitative differences in the GW waveforms computed at different resolutions, the qualitative features discussed here are

robust across all simulations. Unless otherwise specified, we discuss results from simulations using the fiducial grid resolution (with grid spacing  $\Delta x \simeq 184.6 \text{ m}$  in the finest refinement level). The grid structure for the simulations is described in detail in Radice et al. (2018a) and Radice et al. (2016b) for the quasi-circular and eccentric simulations, respectively.

For a clear understanding of the role that high-density deconfinement phase transitions could play in the development of the one-armed spiral instability, we consider a total of 7 EOS models and run a total of 8 simulations with varying phase transition features. In particular, the size of the energy density gap which separates the hadronic and quark phases is a useful way to classify hybrid hadron-quark EOS models and provides a qualitative measure of the ‘strength’ of the phase transition (Alford & Han 2016). As such, we consider EOS models that cover several sizes of the energy density gap, ranging from non-existent (i.e., a purely hadronic EOS) to large, while maintaining consistency with current astrophysical constraints on the dense matter EOS. We consider both phenomenological EOS models (Paschalidis et al. 2018; Alvarez-Castillo & Blaschke 2017; Alford & Sedrakian 2017; Bozzola et al. 2019; Espino & Paschalidis 2022) (in the form of piecewise polytropic approximations using the prescription of Read et al. (2009)) and microphysical, finite temperature EOS models (Bastian 2021; Bombaci & Logoteta 2018; Logoteta et al. 2021; Prakash et al. 2021). We only consider equal-mass ratio binary configurations, with the total binary mass ranging from  $2.6 M_{\odot} - 2.7 M_{\odot}$ . The lack of  $\pi$ -rotational symmetry in BNS configurations with unequal-masses may be a suitable way of effectively seeding non-axisymmetric fluid instabilities that can take hold in the post-merger environment. Neutrino emission and reabsorption are not included for binaries in eccentric orbits, while all quasi-circular binaries include a neutrino treatment via the moment based M0 scheme (Radice et al. 2018a). However, neutrinos are not expected to influence the dynamics on the time scales considered in our study (Radice et al. 2020, 2022). Additionally, magnetic fields are not accounted for in any of our simulations, but these are also expected to be subdominant (Palenzuela et al. 2022). We find that, despite the diversity in binary properties and differences in the evolution, the effects presented in this work are robust.

## 3. RESULTS

The one-armed spiral instability is a non-axisymmetric mode in a rapidly rotating fluid which, when saturated, leads to the dominance of a single

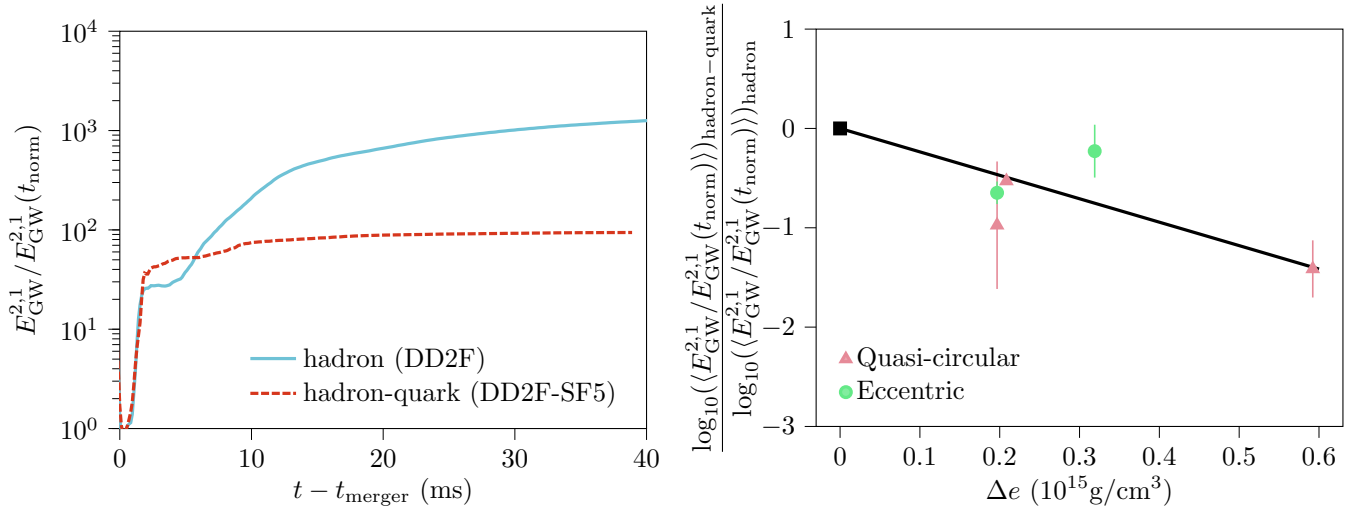


**Figure 1.** *Left panel:* Energy carried by GWs in the  $l = 2, m = 1$  mode as a function of time, scaled by the value at a fixed normalization time  $t_{\text{norm}} = t_{\text{mer}} + 0.5$  ms. The development of the one-armed spiral instability can be observed in the purely hadronic simulation as the energy in the  $l = 2, m = 1$  GW mode continues to grow, but is suppressed in the hadron-quark simulation. *Right panel:* The same quantity depicted in the left panel, but time-averaged over a fixed time window and shown as a function of the energy density gap  $\Delta e$  for each simulation. We normalize by the same quantity for the complementary hadronic EOS. We include approximate error bars, obtained using lower resolution simulations, to represent the uncertainty introduced by our numerical methods. The black solid line represents a linear fit to the data from our simulations. We find that the normalized energy emitted by the  $l = 2, m = 1$  GW mode decreases for simulations that employ EOS models with larger values of  $\Delta e$ .

high-density mode in the fluid density which is displaced from the fluid barycenter (Pickett et al. 1996; Centrella et al. 2001; Saijo et al. 2002; Ou & Tohline 2006). The one-armed spiral instability has been observed to develop commonly in BNS merger simulations that produce long-lived, massive post-merger remnants on timescales of  $\mathcal{O}(10\text{ms})$  (Paschalidis et al. 2015; East et al. 2016; East et al. 2016; Radice et al. 2016a; Lehner et al. 2016) and in simulations of many other astrophysical systems including supernovae (Ott et al. 2005; Kuroda et al. 2014), white dwarfs (Kashyap et al. 2015, 2017) and accretion disks (Kashyap et al. 2017; Wessel et al. 2021). Each fluid density mode that arises during the evolution of a massive NS remnant is associated with GW emission at characteristic frequencies stemming from its pattern speed. As such, the development of the one-armed spiral instability in astrophysical systems may be observed by considering multimodal GW spectroscopy (Radice et al. 2016a). For the simulations considered in this work we extract multimodal GW information within the Newman-Penrose formalism. We compute the coefficients of  $s = -2$  spin-weighted spherical harmonic decompositions of the Newman-Penrose scalar  $\Psi_4$  which we label as  $\Psi_4^{l,m}$ . The one-armed spiral instability can therefore be observed in the GW spectrum extracted from our simulations as a growth in the power and amplitude of the  $l = 2, m = 1$  GW mode

(i.e.,  $\Psi_4^{2,1}$ ) and simultaneous decay of the dominant  $l = 2, m = 2$  GW mode (i.e.,  $\Psi_4^{2,2}$ ).

Our simulations show that *high-density deconfinement phase transitions act to suppress the one-armed spiral instability*. Depending on the features of the phase transition, the one-armed spiral mode may either arise on a significantly longer timescale when compared to simulations which employ purely hadronic EOS models, or it may be suppressed altogether on the timescales probed by our simulations. There are several potential mechanisms via which the instability may be suppressed. For example, it has been shown that the physical extent of the remnant plays an important role in the development of the instability, with larger remnants being more conducive to the development of the instability on shorter timescales (Radice et al. 2016a; Lehner et al. 2016; Saijo & Yoshida 2016; Saijo 2018). The significant softening at high densities introduced by the phase transition results in more compact post-merger remnants (relative to scenarios that consider only hadronic degrees of freedom). As such, the more compact hybrid star remnants may see a weaker development of the one-armed spiral instability when compared to neutron star remnants.

In the left panel of Fig. 1 we show the energy carried by the  $l = 2, m = 1$  GW mode (scaled by the energy emitted at a time shortly after the merger  $t_{\text{norm}} = t_{\text{mer}} + 0.5$  ms) as a function of time for simulations employing the DD2F (hadronic) and DD2F-SF5 (hybrid

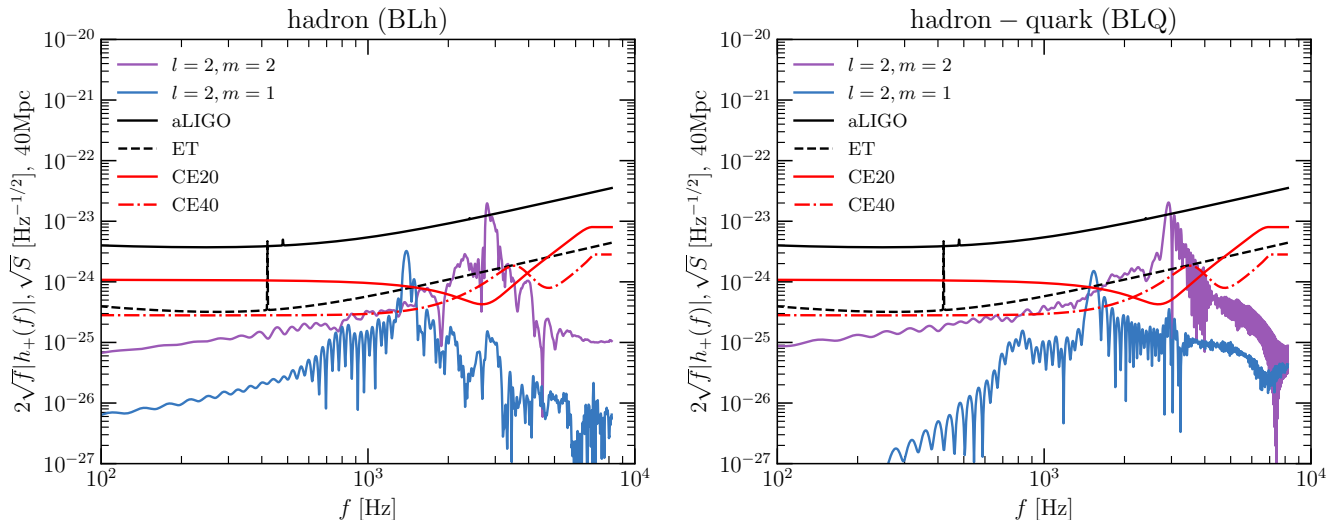


**Figure 2.** Multimodal GW amplitude spectrum computed for symmetric binaries of total mass  $M = 2.6 M_{\odot}$  in an edge-on configuration. Also shown are the noise sensitivity curves for advanced LIGO (aLIGO), Einstein Telescope (ET), the 20 km postmerger-optimized configuration for the Cosmic Explorer (CE20) and the 40 km configuration for Cosmic Explorer (CE40). A suppression in the amplitude spectral density (ASD) as a result of the deconfinement phase transition may be detectable with the third generation detectors and most cleanly with CE40.

hadron-quark) EOSs. We find that the energy carried in the  $l = 2, m = 1$  mode of the GWs is significantly smaller in the simulation employing a hybrid hadron-quark EOS, indicating that the one-armed spiral instability is suppressed in scenarios with deconfinement phase transitions at densities relevant for BNS mergers. We emphasize that in the left panel of Fig. 1 we showcase results for a set of EOS models which are identical below the threshold for a phase transition, and as such the simulations have identical initial conditions. In the right panel of Fig. 1, we show the time-averaged energy emitted by the  $l = 2, m = 1$  GW mode  $\langle E_{\text{GW}}^{2,1} \rangle$  (again scaled by the energy emitted at a time shortly after the merger  $t_{\text{norm}} = t_{\text{mer}} + 0.5 \text{ ms}$ ) as a function of the energy density gap  $\Delta e$ , where we define the energy density gap as the difference between the energy density  $e$  at the end of the hadronic phase and beginning of the quark phase for cold matter in  $\beta$ -equilibrium (Alford & Han 2016),

$$\Delta e \equiv e_{\text{quark,initial}} - e_{\text{hadron,final}}, \quad (1)$$

where we assume units where the speed of light  $c = 1$ . We identify the end and beginning of each phase by considering the change in the approximate adiabatic index  $\Gamma = d \log p / d \log(\rho)$ , where  $p$  is the fluid pressure of the cold, beta-equilibrium, barotropic EOS for each EOS model considered. The region corresponding to the phase transition is always unambiguously marked by discontinuities in, or sudden changes in the slope of, the adiabatic index for the EOS models we consider. For the results depicted in the right panel of Fig. 1, we time-average over a window of  $\Delta t \approx 40 \text{ ms}$  after the

merger except for cases that lead to a remnant collapse on shorter timescales (in such cases, we time-average until the collapse of the NS remnant). Additionally, for each simulation, we normalize by a complementary simulation that uses identical initial data but employs a hadronic EOS having the same low-density behavior below the phase transition threshold as the hybrid hadron-quark EOS. As such, we depict the point corresponding to all hadronic EOS simulations with a black square at  $\Delta e = 0$ . Each simulation is time-averaged to the same extent as its complementary hadronic simulation. We find an anti-correlation between the energy carried in the  $l = 2, m = 1$  GW mode and the size of the energy density gap. In other words, as the size of the energy density gap (and thereby the qualitative ‘strength’ of the phase transition) increases, GW emission in the  $l = 2, m = 1$  mode decreases, which signifies that the one-armed spiral instability is further suppressed for EOS models with ‘stronger’ deconfinement phase transitions. We elaborate on the choice of quantities depicted in Fig. 1 in App. A.

#### 4. DISCUSSION

The characteristic frequency associated with peak emission in the  $l = 2, m = 1$  GW mode has half the value of that associated with the  $l = 2, m = 2$  mode (i.e.,  $f_{\text{peak}}^{2,1} = f_{\text{peak}}^{2,2}/2$ ). Observationally, a GW signal would contain information at all contributing frequencies. However, the dominant GW emission associated with binary coalescence is always expected to be from the  $l = 2, m = 2$  contribution, such that  $f_{\text{peak}} = f_{\text{peak}}^{2,2}$ .

Therefore, a potential observational signature of the one-armed spiral instability is the growth in power of an incoming GW signal at a frequency that is half of the dominant frequency; if it develops in the post-merger environment, the one-armed spiral instability will continuously power the emission of GWs at  $f_{\text{peak}}/2$ , while emission in the dominant  $f_{\text{peak}}$  decays in time (Bernuzzi et al. 2015).

In Fig. 2 we show the post-merger GW amplitude spectrum density (ASD) for a symmetric, edge-on binary situated at a distance of 40 Mpc, which is consistent with the luminosity distance observed for GW170817 (Abbott et al. 2017b). The edge-on configuration is the most optimal for the detection of an  $m = 1$  mode. As expected, we see a relative suppression of power in the  $m = 1$  mode (with respect to the complementing hadronic simulation) with the onset of a deconfinement phase transition. In this realistic configuration, coupled with the 40 km Cosmic Explorer detector (Reitze et al. 2019), the appearance of quarks in the post-merger remnant results in a suppression of the postmerger signal-to-noise ratio (SNR) of the ( $l = 2, m = 1$ ) mode by a factor of 2, from 2.14 in the hadronic case to 1.08 in the hadron-quark case. The GW ASD peak of the  $l = 2, m = 1$  mode (between 1-2 kHz) and the postmerger ASD peak of the  $l = 2, m = 2$  mode (between 2-4 kHz), lie respectively in the most sensitive regions of the 40 km and the 20 km postmerger optimized Cosmic Explorer configurations. Our analysis recommends an increase in detector sensitivities in the high-frequency regimes (see also Zhang et al. (2022)) for best possible constraints on deconfinement phase transitions in BNS mergers.

In this letter we have highlighted, for the first time, that high-density deconfinement phase transitions act to suppress the one-armed spiral instability. We find an anti-correlation between the energy carried in the  $l = 2, m = 1$  GW mode and the size of the energy density gap which qualitatively separates the hadronic and quark phases. Our findings reveal a deep connection between observable multimodal GW emission and the microphysical description of matter in the post-merger environment. We expect the one-armed spiral instability to be detectable at distances of 40 Mpc using future generation detectors (Radice et al. 2016a). If evidence of a strong one-armed spiral mode can be inferred from GW observations of the post-BNS merger environment, our findings suggest that a strong high-density deconfinement phase transition at the densities relevant to BNS mergers would be disfavored. On the other hand, if evidence for the one-armed spiral instability is *not* found for close-by BNS mergers, this could also point to the

possibility of a deconfinement phase transition taking place at densities relevant to BNS mergers.

We point out that other effects relevant in the post-merger environment - such as the presence of strong magnetic fields (Franci et al. 2013) and additional degrees of freedom that can cause a sudden softening of the EOS - may affect the development of the one-armed spiral instability. However, the relevant timescales and extent to which the aforementioned phenomena can affect the development of non-axisymmetric instabilities or the GW spectrum remains uncertain (Radice et al. 2016a; Muhlberger et al. 2014), and may not impact our conclusions (Palenzuela et al. 2022; Zappa et al. 2022). The effects discussed in the present work arise on dynamical timescales  $\sim \mathcal{O}(10\text{ms})$ , and may be the dominant mechanism for suppression of the one-armed spiral instability. Additionally, although we find a trend in the decrease of energy carried by the  $l = 2, m = 1$  GW mode for larger values of  $\Delta e$ , additional studies will help establish a more robust trend and provide an understanding of the potential spread in the trend. In particular, future lines of investigation will include: (1) considering the combined effects of the mass ratio and high-density phase transitions on the development of the one-armed spiral instability; (2) considering the effects of accurate neutrino transport on high-density deconfinement phase transitions, as neutrinos may modify the composition of matter and thereby potentially affect the onset of the phase transition; (3) employing EOS models at systematically increasing values of  $\Delta e$  while holding the hadronic region of the EOS fixed, as a limitation of the present work is the assumption that the  $l = 2, m = 1$  GW mode is perfectly known in the case of hadronic EOSs; and (4) investigating the effects discussed in this work in scenarios with a *crossover* to quark matter, as our present work only considers EOS models with phase transitions. We leave such studies to future work.

PE acknowledges funding from the National Science Foundation under Grant No. PHY-2020275. DR acknowledges funding from the U.S. Department of Energy, Office of Science, Division of Nuclear Physics under Award Number(s) DE-SC0021177 and from the National Science Foundation under Grants No. PHY-2011725, PHY-2116686, and AST-2108467. Simulations were performed on Bridges2 and Expanse (NSF XSEDE allocation TG-PHY160025). This research used resources of the National Energy Research Scientific Computing Center, a DOE Office of Science User Facility supported by the Office of Science of the U.S. Department of Energy under Contract No. DE-AC02-05CH11231.

## REFERENCES

- Abbott, B. P., et al. 2017a, *Astrophys. J. Lett.*, 851, L16, doi: [10.3847/2041-8213/aa9a35](https://doi.org/10.3847/2041-8213/aa9a35)
- . 2017b, *Phys. Rev. Lett.*, 119, 161101
- . 2018, *Phys. Rev. Lett.*, 121, 161101, doi: [10.1103/PhysRevLett.121.161101](https://doi.org/10.1103/PhysRevLett.121.161101)
- . 2019, *Phys. Rev. X*, 9, 011001, doi: [10.1103/PhysRevX.9.011001](https://doi.org/10.1103/PhysRevX.9.011001)
- Ackley, K., et al. 2020, *Publ. Astron. Soc. Austral.*, 37, e047, doi: [10.1017/pasa.2020.39](https://doi.org/10.1017/pasa.2020.39)
- Alford, M., & Sedrakian, A. 2017, *Phys. Rev. Lett.*, 119, 161104, doi: [10.1103/PhysRevLett.119.161104](https://doi.org/10.1103/PhysRevLett.119.161104)
- Alford, M. G., & Han, S. 2016, *Eur. Phys. J. A*, 52, 62, doi: [10.1140/epja/i2016-16062-9](https://doi.org/10.1140/epja/i2016-16062-9)
- Alvarez-Castillo, D. E., & Blaschke, D. B. 2017, *Phys. Rev. C*, 96, 045809, doi: [10.1103/PhysRevC.96.045809](https://doi.org/10.1103/PhysRevC.96.045809)
- Annala, E., Gorda, T., Katerini, E., et al. 2022, *Phys. Rev. X*, 12, 011058, doi: [10.1103/PhysRevX.12.011058](https://doi.org/10.1103/PhysRevX.12.011058)
- Bastian, N.-U. F. 2021, *Phys. Rev. D*, 103, 023001, doi: [10.1103/PhysRevD.103.023001](https://doi.org/10.1103/PhysRevD.103.023001)
- Bauswein, A., Bastian, N.-U. F., Blaschke, D. B., et al. 2019, *Phys. Rev. Lett.*, 122, 061102, doi: [10.1103/PhysRevLett.122.061102](https://doi.org/10.1103/PhysRevLett.122.061102)
- Bauswein, A., Baumgarte, T. W., & Janka, H. T. 2013, *Phys. Rev. Lett.*, 111, 131101, doi: [10.1103/PhysRevLett.111.131101](https://doi.org/10.1103/PhysRevLett.111.131101)
- Bauswein, A., Blacker, S., Lioutas, G., et al. 2021, *Phys. Rev. D*, 103, 123004, doi: [10.1103/PhysRevD.103.123004](https://doi.org/10.1103/PhysRevD.103.123004)
- Bauswein, A., Just, O., Janka, H.-T., & Stergioulas, N. 2017, *Astrophys. J. Lett.*, 850, L34, doi: [10.3847/2041-8213/aa9994](https://doi.org/10.3847/2041-8213/aa9994)
- Bauswein, A., Blacker, S., Vijayan, V., et al. 2020, *Phys. Rev. Lett.*, 125, 141103, doi: [10.1103/PhysRevLett.125.141103](https://doi.org/10.1103/PhysRevLett.125.141103)
- Bernuzzi, S., Dietrich, T., & Nagar, A. 2015, *Phys. Rev. Lett.*, 115, 091101, doi: [10.1103/PhysRevLett.115.091101](https://doi.org/10.1103/PhysRevLett.115.091101)
- Blacker, S., Bastian, N.-U. F., Bauswein, A., et al. 2020, *Phys. Rev. D*, 102, 123023, doi: [10.1103/PhysRevD.102.123023](https://doi.org/10.1103/PhysRevD.102.123023)
- Bombaci, I., & Logoteta, D. 2018, *Astron. Astrophys.*, 609, A128, doi: [10.1051/0004-6361/201731604](https://doi.org/10.1051/0004-6361/201731604)
- Bozzola, G., Espino, P. L., Lewin, C. D., & Paschalidis, V. 2019. <https://arxiv.org/abs/1905.00028>
- Breschi, M., Bernuzzi, S., Godzieba, D., Perego, A., & Radice, D. 2022, *Phys. Rev. Lett.*, 128, 161102, doi: [10.1103/PhysRevLett.128.161102](https://doi.org/10.1103/PhysRevLett.128.161102)
- Breschi, M., Perego, A., Bernuzzi, S., et al. 2021, *Mon. Not. Roy. Astron. Soc.*, 505, 1661, doi: [10.1093/mnras/stab1287](https://doi.org/10.1093/mnras/stab1287)
- Capano, C. D., Tews, I., Brown, S. M., et al. 2020, *Nature Astron.*, 4, 625, doi: [10.1038/s41550-020-1014-6](https://doi.org/10.1038/s41550-020-1014-6)
- Centrella, J. M., New, K. C. B., Lowe, L. L., & Brown, J. D. 2001, *Astrophys. J. Lett.*, 550, L193, doi: [10.1086/319634](https://doi.org/10.1086/319634)
- Coughlin, M. W., Dietrich, T., Margalit, B., & Metzger, B. D. 2019, *Mon. Not. Roy. Astron. Soc.*, 489, L91, doi: [10.1093/mnras/slz133](https://doi.org/10.1093/mnras/slz133)
- Damour, T., Nagar, A., & Villain, L. 2012, *Phys. Rev. D*, 85, 123007, doi: [10.1103/PhysRevD.85.123007](https://doi.org/10.1103/PhysRevD.85.123007)
- De, S., Finstad, D., Lattimer, J. M., et al. 2018, *Phys. Rev. Lett.*, 121, 091102, doi: [10.1103/PhysRevLett.121.091102](https://doi.org/10.1103/PhysRevLett.121.091102)
- Dietrich, T., Coughlin, M. W., Pang, P. T. H., et al. 2020, *Science*, 370, 1450, doi: [10.1126/science.abb4317](https://doi.org/10.1126/science.abb4317)
- East, W. E., Paschalidis, V., & Pretorius, F. 2016, *Class. Quant. Grav.*, 33, 244004, doi: [10.1088/0264-9381/33/24/244004](https://doi.org/10.1088/0264-9381/33/24/244004)
- East, W. E., Paschalidis, V., Pretorius, F., & Shapiro, S. L. 2016, *prd*, 93, 024011, doi: [10.1103/PhysRevD.93.024011](https://doi.org/10.1103/PhysRevD.93.024011)
- Espino, P. L., & Paschalidis, V. 2022, *Phys. Rev. D*, 105, 043014, doi: [10.1103/PhysRevD.105.043014](https://doi.org/10.1103/PhysRevD.105.043014)
- Espino, P. L., Paschalidis, V., Baumgarte, T. W., & Shapiro, S. L. 2019, *Phys. Rev. D*, 100, 043014, doi: [10.1103/PhysRevD.100.043014](https://doi.org/10.1103/PhysRevD.100.043014)
- Evans, M., et al. 2021, arXiv. <https://arxiv.org/abs/2109.09882>
- Franci, L., De Pietri, R., Dionysopoulou, K., & Rezzolla, L. 2013, *Phys. Rev. D*, 88, 104028, doi: [10.1103/PhysRevD.88.104028](https://doi.org/10.1103/PhysRevD.88.104028)
- Fujimoto, Y., Fukushima, K., Hotokezaka, K., & Kyutoku, K. 2022, arXiv. <https://arxiv.org/abs/2205.03882>
- Gourgoulhon, E., Grandclement, P., Taniguchi, K., Marck, J.-A., & Bonazzola, S. 2001, *Phys. Rev. D*, 63, 064029, doi: [10.1103/PhysRevD.63.064029](https://doi.org/10.1103/PhysRevD.63.064029)
- Hinderer, T., Lackey, B. D., Lang, R. N., & Read, J. S. 2010, *Phys. Rev. D*, 81, 123016, doi: [10.1103/PhysRevD.81.123016](https://doi.org/10.1103/PhysRevD.81.123016)
- Hotokezaka, K., Kyutoku, K., Okawa, H., Shibata, M., & Kiuchi, K. 2011, *Phys. Rev. D*, 83, 124008, doi: [10.1103/PhysRevD.83.124008](https://doi.org/10.1103/PhysRevD.83.124008)
- Kashyap, R., Fisher, R., García-Berro, E., et al. 2015, *Astrophys. J.*, 800, L7, doi: [10.1088/2041-8205/800/1/17](https://doi.org/10.1088/2041-8205/800/1/17)
- . 2017, *Astrophys. J.*, 840, 16, doi: [10.3847/1538-4357/aa6afb](https://doi.org/10.3847/1538-4357/aa6afb)
- Kashyap, R., et al. 2022, *Phys. Rev. D*, 105, 103022, doi: [10.1103/PhysRevD.105.103022](https://doi.org/10.1103/PhysRevD.105.103022)
- Kedia, A., Kim, H. I., Suh, I.-S., & Mathews, G. J. 2022, arXiv. <https://arxiv.org/abs/2203.05461>
- Kuroda, T., Takiwaki, T., & Kotake, K. 2014, *Phys. Rev. D*, 89, 044011, doi: [10.1103/PhysRevD.89.044011](https://doi.org/10.1103/PhysRevD.89.044011)

- Lee, W. H., Ramirez-Ruiz, E., & van de Ven, G. 2010, *Astrophys. J.*, 720, 953, doi: [10.1088/0004-637X/720/1/953](https://doi.org/10.1088/0004-637X/720/1/953)
- Lehner, L., Liebling, S. L., Palenzuela, C., & Motl, P. M. 2016, *Phys. Rev.*, D94, 043003, doi: [10.1103/PhysRevD.94.043003](https://doi.org/10.1103/PhysRevD.94.043003)
- Liebling, S. L., Palenzuela, C., & Lehner, L. 2021, *Class. Quant. Grav.*, 38, 115007, doi: [10.1088/1361-6382/abf898](https://doi.org/10.1088/1361-6382/abf898)
- Loffredo, E., Perego, A., Logoteta, D., & Branchesi, M. 2022. <https://arxiv.org/abs/2209.04458>
- Logoteta, D. 2021, *Universe*, 7, 408, doi: [10.3390/universe7110408](https://doi.org/10.3390/universe7110408)
- Logoteta, D., Perego, A., & Bombaci, I. 2021, *Astron. Astrophys.*, 646, A55, doi: [10.1051/0004-6361/202039457](https://doi.org/10.1051/0004-6361/202039457)
- Lovato, A., et al. 2022. <https://arxiv.org/abs/2211.02224>
- Margalit, B., & Metzger, B. D. 2017, *Astrophys. J. Lett.*, 850, L19, doi: [10.3847/2041-8213/aa991c](https://doi.org/10.3847/2041-8213/aa991c)
- Most, E. R., Jens Papenfort, L., Dexheimer, V., et al. 2020, *Eur. Phys. J. A*, 56, 59
- Most, E. R., Papenfort, L. J., Dexheimer, V., et al. 2019, *Phys. Rev. Lett.*, 122, 061101, doi: [10.1103/PhysRevLett.122.061101](https://doi.org/10.1103/PhysRevLett.122.061101)
- Muhlberger, C. D., Nouri, F. H., Duez, M. D., et al. 2014, *Phys. Rev. D*, 90, 104014, doi: [10.1103/PhysRevD.90.104014](https://doi.org/10.1103/PhysRevD.90.104014)
- Ott, C. D., Ou, S., Tohline, J. E., & Burrows, A. 2005, *Astrophys. J. Lett.*, 625, L119, doi: [10.1086/431305](https://doi.org/10.1086/431305)
- Ou, S., & Tohline, J. 2006, *Astrophys. J.*, 651, 1068, doi: [10.1086/507597](https://doi.org/10.1086/507597)
- Palenzuela, C., Aguilera-Miret, R., Carrasco, F., et al. 2022, *Phys. Rev. D*, 106, 023013, doi: [10.1103/PhysRevD.106.023013](https://doi.org/10.1103/PhysRevD.106.023013)
- Pang, P. T. H., Tews, I., Coughlin, M. W., et al. 2021, *Astrophys. J.*, 922, 14, doi: [10.3847/1538-4357/ac19ab](https://doi.org/10.3847/1538-4357/ac19ab)
- Paschalidis, V., East, W. E., Pretorius, F., & Shapiro, S. L. 2015, *Phys. Rev.*, D92, 121502, doi: [10.1103/PhysRevD.92.121502](https://doi.org/10.1103/PhysRevD.92.121502)
- Paschalidis, V., Yagi, K., Alvarez-Castillo, D., Blaschke, D. B., & Sedrakian, A. 2018, *Phys. Rev.*, D97, 084038, doi: [10.1103/PhysRevD.97.084038](https://doi.org/10.1103/PhysRevD.97.084038)
- Perego, A., Bernuzzi, S., & Radice, D. 2019, *Eur. Phys. J. A*, 55, 124, doi: [10.1140/epja/i2019-12810-7](https://doi.org/10.1140/epja/i2019-12810-7)
- Perego, A., Logoteta, D., Radice, D., et al. 2022, *Phys. Rev. Lett.*, 129, 032701, doi: [10.1103/PhysRevLett.129.032701](https://doi.org/10.1103/PhysRevLett.129.032701)
- Pickett, B. K., Durisen, R. H., & Davis, G. A. 1996, *ApJ*, 458, 714, doi: [10.1086/176852](https://doi.org/10.1086/176852)
- Pollney, D., Reisswig, C., Schnetter, E., Dorband, N., & Diener, P. 2011, *Phys. Rev. D*, 83, 044045, doi: [10.1103/PhysRevD.83.044045](https://doi.org/10.1103/PhysRevD.83.044045)
- Prakash, A., Radice, D., Logoteta, D., et al. 2021, *Phys. Rev. D*, 104, 083029, doi: [10.1103/PhysRevD.104.083029](https://doi.org/10.1103/PhysRevD.104.083029)
- Punturo, M., et al. 2010, *Class. Quant. Grav.*, 27, 194002, doi: [10.1088/0264-9381/27/19/194002](https://doi.org/10.1088/0264-9381/27/19/194002)
- Radice, D., Bernuzzi, S., Del Pozzo, W., Roberts, L. F., & Ott, C. D. 2017, *Astrophys. J. Lett.*, 842, L10, doi: [10.3847/2041-8213/aa775f](https://doi.org/10.3847/2041-8213/aa775f)
- Radice, D., Bernuzzi, S., & Ott, C. D. 2016a, *Phys. Rev.*, D94, 064011, doi: [10.1103/PhysRevD.94.064011](https://doi.org/10.1103/PhysRevD.94.064011)
- Radice, D., Bernuzzi, S., & Perego, A. 2020, *Ann. Rev. Nucl. Part. Sci.*, 70, 95, doi: [10.1146/annurev-nucl-013120-114541](https://doi.org/10.1146/annurev-nucl-013120-114541)
- Radice, D., Bernuzzi, S., Perego, A., & Haas, R. 2022, *Mon. Not. Roy. Astron. Soc.*, 512, 1499, doi: [10.1093/mnras/stac589](https://doi.org/10.1093/mnras/stac589)
- Radice, D., & Dai, L. 2019, *Eur. Phys. J. A*, 55, 50, doi: [10.1140/epja/i2019-12716-4](https://doi.org/10.1140/epja/i2019-12716-4)
- Radice, D., Galeazzi, F., Lippuner, J., et al. 2016b, *Mon. Not. Roy. Astron. Soc.*, 460, 3255, doi: [10.1093/mnras/stw1227](https://doi.org/10.1093/mnras/stw1227)
- Radice, D., Perego, A., Hotokezaka, K., et al. 2018a, *Astrophys. J.*, 869, 130, doi: [10.3847/1538-4357/aaf054](https://doi.org/10.3847/1538-4357/aaf054)
- Radice, D., Perego, A., Zappa, F., & Bernuzzi, S. 2018b, *Astrophys. J. Lett.*, 852, L29, doi: [10.3847/2041-8213/aaa402](https://doi.org/10.3847/2041-8213/aaa402)
- Radice, D., & Rezzolla, L. 2012, *Astron. Astrophys.*, 547, A26, doi: [10.1051/0004-6361/201219735](https://doi.org/10.1051/0004-6361/201219735)
- Radice, D., Rezzolla, L., & Galeazzi, F. 2014a, *Mon. Not. Roy. Astron. Soc.*, 437, L46, doi: [10.1093/mnrasl/slt137](https://doi.org/10.1093/mnrasl/slt137)
- . 2014b, *Class. Quant. Grav.*, 31, 075012, doi: [10.1088/0264-9381/31/7/075012](https://doi.org/10.1088/0264-9381/31/7/075012)
- Read, J. S., Lackey, B. D., Owen, B. J., & Friedman, J. L. 2009, *Phys. Rev. D*, 79, 124032, doi: [10.1103/PhysRevD.79.124032](https://doi.org/10.1103/PhysRevD.79.124032)
- Reitze, D., et al. 2019, *Bull. Am. Astron. Soc.*, 51, 035. <https://arxiv.org/abs/1907.04833>
- Saijo, M. 2018, *Phys. Rev. D*, 98, 024003
- Saijo, M., Baumgarte, T. W., & Shapiro, S. L. 2002, *Astrophys. J.*, 595, 352, doi: [10.1086/377334](https://doi.org/10.1086/377334)
- Saijo, M., & Yoshida, S. 2016, *Phys. Rev. D*, 94, 084032
- Schnetter, E., Hawley, S. H., & Hawke, I. 2004, *Class. Quant. Grav.*, 21, 1465, doi: [10.1088/0264-9381/21/6/014](https://doi.org/10.1088/0264-9381/21/6/014)
- Sekiguchi, Y., Kiuchi, K., Kyutoku, K., & Shibata, M. 2011, *Phys. Rev. Lett.*, 107, 211101, doi: [10.1103/PhysRevLett.107.211101](https://doi.org/10.1103/PhysRevLett.107.211101)
- Shibata, M. 2005, *Phys. Rev. Lett.*, 94, 201101, doi: [10.1103/PhysRevLett.94.201101](https://doi.org/10.1103/PhysRevLett.94.201101)
- Taniguchi, K., &ourgoulhon, E. 2002, *Phys. Rev. D*, 65, 044027, doi: [10.1103/PhysRevD.65.044027](https://doi.org/10.1103/PhysRevD.65.044027)

- Taniguchi, K., Gourgoulhon, E., & Bonazzola, S. 2001, Phys. Rev. D, 64, 064012, doi: [10.1103/PhysRevD.64.064012](https://doi.org/10.1103/PhysRevD.64.064012)
- Tootle, S., Ecker, C., Topolski, K., et al. 2022, arXiv. <https://arxiv.org/abs/2205.05691>
- Weih, L. R., Hanauske, M., & Rezzolla, L. 2020, Phys. Rev. Lett., 124, 171103, doi: [10.1103/PhysRevLett.124.171103](https://doi.org/10.1103/PhysRevLett.124.171103)
- Wessel, E., Paschalidis, V., Tsokaros, A., Ruiz, M., & Shapiro, S. L. 2021, Phys. Rev. D, 103, 043013, doi: [10.1103/PhysRevD.103.043013](https://doi.org/10.1103/PhysRevD.103.043013)
- York, Jr., J. W. 1999, Phys. Rev. Lett., 82, 1350, doi: [10.1103/PhysRevLett.82.1350](https://doi.org/10.1103/PhysRevLett.82.1350)
- Zappa, F., Bernuzzi, S., Radice, D., & Perego, A. 2022. <https://arxiv.org/abs/2210.11491>
- Zhang, T., Yang, H., Martynov, D., Schmidt, P., & Miao, H. 2022. <https://arxiv.org/abs/2212.12144>
- Zlochower, Y., Brandt, S. R., Diener, P., et al. 2022, The Einstein Toolkit, The "Berhard Riemann" release, ET\_2022\_05, Zenodo, doi: [10.5281/zenodo.6588641](https://doi.org/10.5281/zenodo.6588641)



## APPENDIX

## A. GW PROBE OF THE ONE-ARMED SPIRAL INSTABILITY

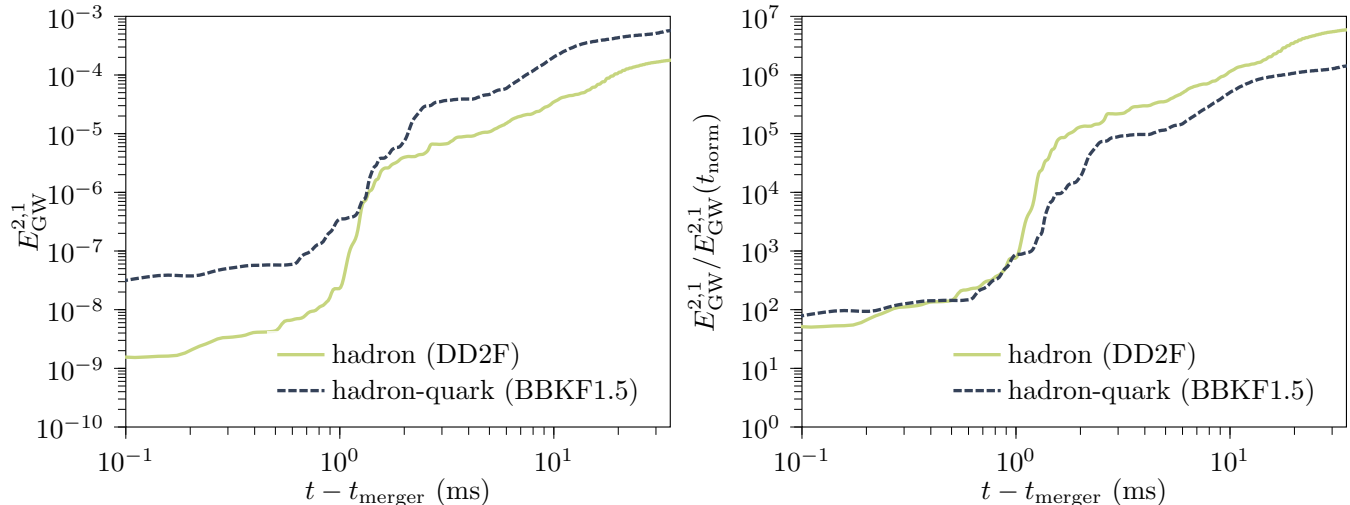


**Figure 3.** *Left panel:* Energy in the  $l = 2, m = 1$  GW mode as a function of time for simulations employing a hadronic (DD2F) and hadron-quark (BBKF1.5) EOS; the simulations use identical initial conditions and are run with a grid resolution of  $\Delta x = 369.2$  m in the finest grid. These results showcase that the one-armed spiral instability may be seeded at different levels in the postmerger environment for different simulations. *Right panel:* Same quantity as the left panel, but normalized to the value at a time shortly after merger,  $t_{\text{norm}} = t_{\text{merger}} + 0.5$  ms. Normalizing at this time accounts for the one-armed spiral instability being seeded at disparate levels across simulations.

In Fig. 1 we depict an example of GW quantities that exhibit the suppression of the one-armed spiral instability for simulations that employ hadron-quark EOSs. In particular, we calculate the GW energy carried in the  $l = 2, m = 1$  mode. In Fig. 1 we show  $E_{\text{GW}}^{2,1}$  normalized to its value at a time shortly after the merger; we depict normalized quantities because of the variable nature in which the one-armed spiral instability is seeded in the immediate post-merger environment in the context of numerical studies. Unless it is explicitly excited as a non-axisymmetric perturbation of a known amplitude (e.g., as a fixed-amplitude perturbation in the rest mass density), the one-armed spiral instability arises numerically from error at the level of floating-point precision (Espino et al. 2019). As such, small differences in the early post-merger evolution of the fluid can result in the instability being seeded at different strengths. We do not explicitly seed the one-armed spiral instability using fluid perturbations in this work and, as a result, simulations that either run on different machines, use different grid resolutions, or use different numerical libraries result in different strengths for the initial instability seed. In Fig. 3 we show the energy in the  $l = 2, m = 1$  GW mode  $E_{\text{GW}}^{2,1}$  as a function of time for a set of low resolution simulations used to produce the error bars of Fig. 1. The left panel of Fig. 3 shows  $E_{\text{GW}}^{2,1}$  as extracted from our simulations and appears to show that the simulation employing a hadron-quark EOS produces a larger energy in the  $l = 2, m = 1$  GW mode. However, it is clear the energy at a time shortly after the merger  $E_{\text{GW}}^{2,1}(t_{\text{merger}} + \epsilon)$  (where  $\epsilon$  is a small additive time) is larger for the hadron-quark simulation, suggesting that the one-armed spiral instability was seeded at a larger amplitude in that case. In order to account for the different levels at which the one-armed spiral instability is seeded in the immediate post-merger environment, we normalize the quantities depicted in Fig. 1 at a time shortly after the merger  $t_{\text{norm}} = t_{\text{mer}} + \epsilon$ . We find that setting  $\epsilon = 0.5$  ms results in all simulations in our work having roughly equal values of  $E_{\text{GW}}^{2,1}$  in the few ms immediately following merger. Normalizing at a time shortly after merger ensures that all simulations have approximate parity in the level at which the one-armed spiral instability is seeded and leads to the robust trend established in the right panel of Fig. 1, regardless of grid resolution used.